

Quasiparticle Excitations and Photoemission Spectra in Solid C₆₀*

Steven G. Louie and Eric L. Shirley

Department of Physics, University of California at Berkeley, Berkeley, CA 94720

and

Materials Sciences Division, Lawrence Berkeley Laboratory, Berkeley, CA 94720 USA

Received July 12, 1993

We report calculations of the electron excitation energies and photoemission spectra in undoped, solid C₆₀ using a quasiparticle self-energy approach. The effects of electron correlations and molecular orientational disorders are included. We find a quasiparticle band gap of 2.15 eV in agreement with recent experimental data and sizable band dispersions of ~ 1 eV for the highest occupied molecular orbital (HOMO) and the lowest unoccupied molecular orbital (LUMO) band complexes. The calculated angle-resolved inverse photoemission spectra for the LUMO bands exhibit minimal angular dependence, explaining the observed lack of dispersion in the spectral peak positions in recent experimental work on epitaxial thin films. The present results show that, although many-electron corrections to the band gap and dispersion are sizable, the electron excitation energies in undoped fullerenes may be described in a standard quasiparticle band picture with molecular orientational disorder.

I. Introduction

The study of carbon-based materials has become an extraordinarily active field in the past few years. In addition to the fullerenes [1], which are carbon clusters in cage-like structures, many other novel structures of pure carbon have recently been synthesized including the fullerenes [2] (crystals of fullerenes), the buckytubes [3] (graphitic tubules of nanometer-size diameters), and the fullerene onions [4] (concentric fullerenes of different sizes). These systems all have fascinating new properties which are being actively explored. Of the fullerenes, the C₆₀ buckyball [1] is the most symmetric and abundant structure with 60 carbon atoms forming an icosahedral cage of 20 hexagons and 12 pentagons. The discovery of superconductivity [5] in doped solid C₆₀ has led to further rigorous research activity in this field. In particular, the electronic structure of the fullerenes has been the subject of numerous experimental and theoretical investigations. Nonetheless, some of the most fundamental issues still remain unresolved. These include the size of the energy gap, the degree of band dispersion, the nature of electron correlation effects, and the effects of electron correlation

and/or molecular orientation on optical and photoemission properties of this molecular solid.

To address some of these issues, we have carried out calculations on the electron excitation energies in undoped solid C₆₀ using an *ab initio* quasiparticle approach [6]. The approach is based on an expansion of the electron self energy (the many-electron correction to an electron excitation energy) to lowest order in the dynamically screened Coulomb interaction, the so-called GW approximation [7]. We investigated the electronic structure of solid C₆₀ in three different geometric structures: a hypothetical Fm3 structure which has all the molecules identically oriented in an fcc lattice, the lower temperature Pa3 structure [8], and the room temperature randomly oriented structure. Our quasiparticle calculation for the ordered Fm3 structure yielded a direct energy gap of 2.15 eV as opposed to the 1.04 eV band gap obtained in the standard local density functional approximation (LDA) [9]. This is to be compared to a gap of 1.85 ± 0.1 eV from microwave conductivity experiments [10] and 2.3-2.6 eV inferred from direct and inverse photoemission data [11-14]. Moreover, the computed results for the HOMO and LUMO band complexes exhibit a 30% enhancement in band width as compared to those from the LDA.

*Invited talk.

Since the molecules are orientationally disordered at room temperature, we use a Slater-Koster Hamiltonian [15] fit to the $Fm\bar{3}$ quasiparticle band structure to examine the effects of molecular orientation. Complete orientational disorder removes sharp features in the density of states (DOS) but yields little change in the band edges and widths. Moreover, the Slater-Koster Hamiltonian has enabled computation of angle-resolved photoemission spectra (ARPES). In good agreement with experiment [16,17], the calculated spectra reveal little dispersion of the spectral peak positions with angle for several reasons (see below). The issue of the observed apparent lack of dispersion is a subject of current interest and debate. It has been used by some as evidence for nondispersive bands in this material and hence strong electron correlation effects.

The remainder of the paper is organized as follows. In Sec. II, the theoretical methods and some of the computational details are discussed. In Sec. III, we present the calculated results and compare them with experimental data, in particular those from photoemission measurements. Finally, in Sec. IV, a summary and some conclusions are presented.

II. Theoretical Methods and Computational Details

The present study was carried out in four stages to investigate various effects on the electron excitation spectrum of solid C_{60} . First, we performed an ab initio pseudopotential LDA calculation to determine the self-consistent valence charge density in the $Fm\bar{3}$ structure. This also gave the Kohn-Sham one-electron energies and wavefunctions. Next, we carried out a first-principles quasiparticle calculation to obtain the electron excitation energies including many-electron self-energy effects. Subsequently, a Slater-Koster tight-binding Hamiltonian was obtained by fitting to the calculated quasiparticle energies. Using the Slater-Koster Hamiltonian, calculations of the quasiparticle density of states and simulated angle-resolved photoemission spectra were performed. Effects of molecular orientation were included through rotating the molecules in a supercell geometry.

For the LDA calculation, we employed a plane-wave ab initio pseudopotential formalism [18] and the Ceperley-Alder exchange-correlation potential [19]. The carbon norm-conserving pseudopotential was generated using the scheme of Hamann, Schluter and Chiang [20]. Convergent results were obtained with a 48-Ry plane-wave cutoff for the one-electron wavefunctions. In the case of the $Fm\bar{3}$ structure which contains one molecule (60 carbon atoms) per unit cell, this corresponds to 27,000 x 27,000 Hamiltonian matrices to be diagonalized. To make the calculations feasible while still obtaining 2,400 conduction band states required in the evaluation of the electron self energy in the quasiparticle calculation, we adopted a symmetrized-plane-wave basis to block-diagonalize these matrices. Our LDA results are in excellent agreement with previous plane-wave pseudopotential LDA calculations [21].

The quasiparticle calculations were done using the Hybertsen-Louie approach [6]. Because of exchange and correlation effects, the electron excitation energies in a solid can be significantly different from those of one-electron theories. The energies and wavefunctions appropriate for the particle-like excitations in an interacting many electron system are given by the quasiparticle equation [7]:

$$[T + V_{\text{ext}}(\mathbf{r}) + V_H(\mathbf{r})]\psi(\mathbf{r}) + \int d\mathbf{r}' \Sigma(\mathbf{r}, \mathbf{r}'; E^{qp})\psi(\mathbf{r}') = E^{qp} \psi(\mathbf{r}) \quad (1)$$

where T is the kinetic energy operator, V_{ext} the external potential due to the ions, V_H the average electrostatic Hartree potential, and C the electron self-energy operator respectively. The self-energy operator C contains the effects of exchange and dynamical correlations. In general, it is nonlocal, energy-dependent and nonhermitian with the imaginary part giving the lifetime of the quasiparticles.

In the GW approximation, the self-energy operator is expanded to first order in the screened Coulomb interaction:

$$\Sigma(\mathbf{r}, \mathbf{r}'; E) = \frac{i}{2\pi} \int d\omega e^{-i\delta\omega} G(\mathbf{r}, \mathbf{r}'; E - \omega) W(\mathbf{r}, \mathbf{r}'; \omega) . \quad (2)$$

Here, G is the crystalline electron Green's function and W the dynamically screened Coulomb interaction. In

the calculations, the electron Green's function was constructed initially using the LDA Kohn-Sham eigenfunctions and eigenvalues, and subsequently updated with the quasiparticle spectrum from Eq. (1). The dielectric response matrix used to construct the screened Coulomb interaction W was obtained by first calculating the static dielectric matrix using the Levine-Louie-Hybertsen approach.^[22] This dielectric matrix, which includes the local field screening effects, was extended to finite frequencies within a generalized plasmon pole model employing exact dispersion and sum rule relations^[6]. There were no adjustable parameter in the calculations, and the approach has been found to be highly reliable for a wide variety of systems, including diamond and graphite^[6,23]. We estimate the convergence in the calculated values with respect to numerical cutoffs to be a few hundredths of an eV.

Using the calculated quasiparticle results, a Slater-Koster Hamiltonian was constructed with a molecular orbital basis employing the angular character^[21] of the $\ell = 5, 6$ molecular orbitals in the HOMO (H_g), LUMO (T_{1u}) and next higher (T_{1g}) band complexes. This tight-binding Hamiltonian allowed us to study the effects of molecular orientational disorder on the electronic states near the band gap. We found that the important banding effects were restricted to next-neighbor (i.e. next molecule) H_g - H_g, T_{1u} - T_{1u} and T_{1g} - T_{1g} hopping, in agreement with the work by Satpathy et al.^[24] Within each band complex, we included a term energy and parameters for the σ -, π - and δ -hybridization between neighboring molecular orbitals of the same type (e.g., H_g). This Hamiltonian was then used to study the electronic structure of the *Fm3* structure, the low temperature *Pa3* structure, and the room temperature random structure. The room temperature solid was simulated using an ensemble of supercells with periodic Born-von Karman boundary conditions containing up to several thousand randomly oriented C₆₀ molecules. The Haydock recursion method^[25] was used to evaluate the density of states (DOS).

For simulating an angle-resolved direct or inverse photoemission spectrum, a "k-resolved" DOS is computed as follows. Here, although orientational disorder formally destroys all translational symmetry, energy-momentum dispersion is still a meaningful concept if the disorder is a relatively weak perturbation to the to-

tal Hamiltonian. We use the following spectral function to approximate the k-resolved DOS:

$$A_{\mathbf{k},\mathbf{k}}(E) \sim \sum_n \sum_\mu | \langle n\mathbf{k} | \psi_\mu \rangle_S |^2 \delta(E - \epsilon_\mu). \quad (3)$$

Here $|n - \mathbf{k}\rangle$ are Bloch states for an ordered system, while $|\psi_\mu\rangle$ and ϵ_μ are associated with a quasiparticle state μ in the presence of disorder. S denotes integration only over one supercell. For a given \mathbf{k} , such an expression for the unoccupied states should approximately mimic an angle-resolved inverse-photoemission spectrum for a randomly oriented crystal if initial-state DOS effects may be neglected. Also, the short mean-free-path and the presence of a crystal surface in photoemission requires Brillouin-zone integration over the component of \mathbf{k} normal to the surface. We have made these assumptions below in our comparison of the theoretical spectra with photoemission data.

III. Results and Discussions

At room temperature, the C₆₀ molecules condense to form a crystal in a fcc arrangement but with the molecules dynamically randomly oriented. Each molecule is spinning rapidly at a rate of about 10⁹ rotations/second. Fig. 1 shows a model of solid C₆₀ in which all the molecules are oriented the same way. This is the hypothetical *Fm3* structure which has been used extensively as a reference structure in various studies because it contains only one C₆₀ molecule per unit cell. At temperatures below 249 K, the free rotation of the molecules ceases and the solid transforms to a *Pa3* structure which has a simple-cubic unit cell with four molecules in the basis^[8]. The *Pa3* structure may be obtained by taking the *Fm3* structure in Fig. 1 and rotating each of the four molecules in the fcc cubic cell by $\sim 22^\circ$ about a different $\langle 111 \rangle$ axis in a prescribed fashion^[8].

The electronic structure of solid C₆₀ is basically one of a molecular crystal. For an isolated C₆₀ molecule, there are 240 valence electrons or 120 occupied molecular orbitals. The highest occupied molecular orbitals and the lowest unoccupied molecular orbitals are both angular momentum $\ell = 5$ states made up of the π orbitals of the carbon layer. The HOMO is five-fold degenerate and the LUMO is 3-fold degenerate. In the

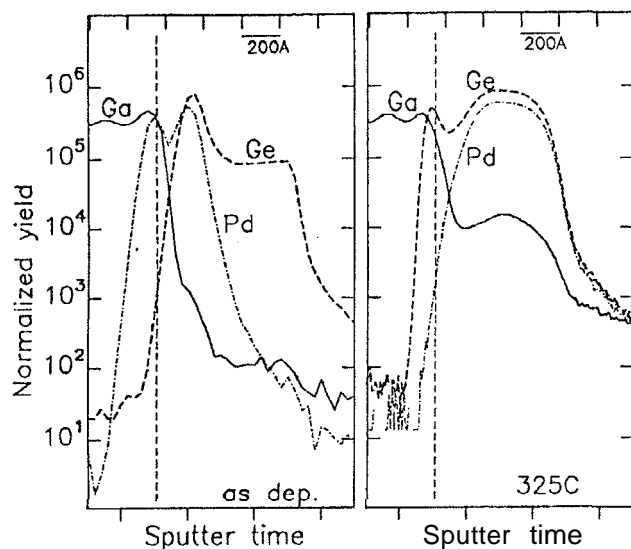


Figure 1: Schematic picture of solid C_{60} in the $Fm3$ structure.

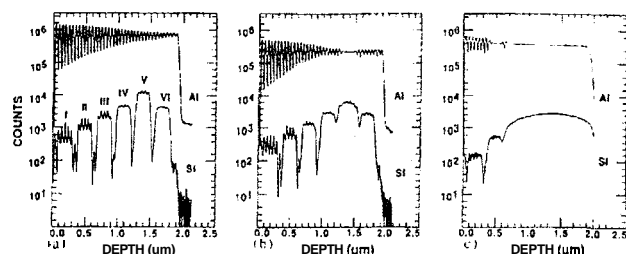


Figure 2: Calculated HOMO (H), LUMO (T_{1u}), and next higher (T_{1g}) bands for undoped, solid C_{60} in the $Fm3$ structure: (a) LDA and (b) quasiparticle results.

$Fm3$ structure, the HOMO's and LUMO's interact to form the HOMO-derived complex of the 5 highest valence bands and the LUMO-derived complex of the 3 lowest conduction bands. LDA calculations give a direct gap material for this structure with a band gap of 1 eV and band dispersion of about 0.5 eV for the HOMO and LUMO complexes.

Figure 2 depicts our calculated quasiparticle HOMO and LUMO bands in the $Fm3$ structure together with the LDA results. Many-electron effects give rise to two major corrections to the LDA results. The energy gap is enlarged by a factor of two from 1.04 eV to 2.15 eV. This enhancement of the gap brings the theoretical result into good agreement with the experimental data (see Table I) and is consistent with trends in previous quasiparticle calculations for semiconductors and insulators. The self-energy operator seen by a quasielectron is very different from that of the quasihole. The many-body effects are not reproduced well by the simple LDA

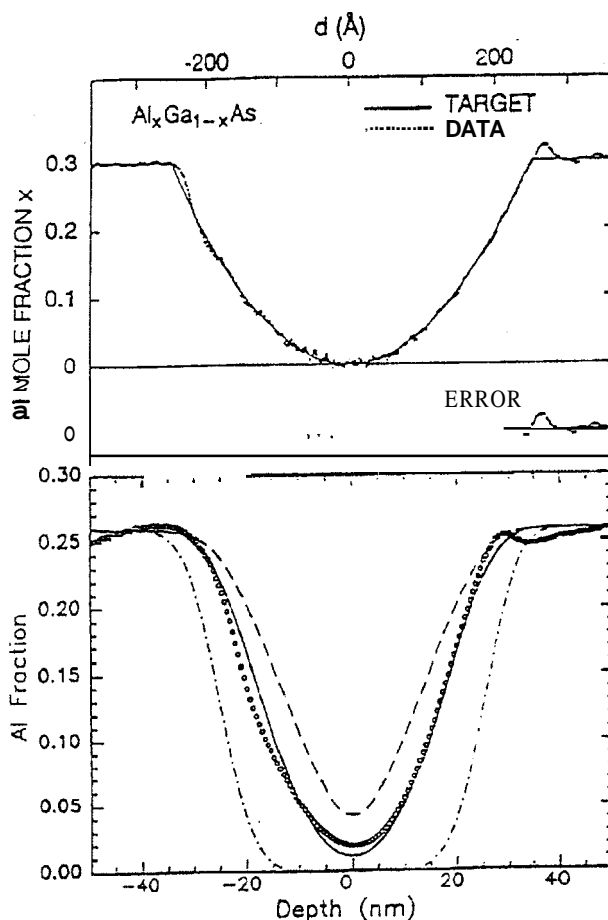


Figure 3: Quasiparticle density of states for solid C_{60} in different orientational configurations.

exchange-correlation potential which depends only on the local electron density. Another notable many-body correction is that the band widths of both the HOMO and LUMO complexes are increased by approximately 30%. As discussed below, this latter correction also has important consequences in interpreting photoemission data.

In Fig. 3, the effects of molecular orientation are demonstrated by contrasting the quasiparticle DOS for the $Fm3$, $Pa3$, and the room temperature randomly oriented structure. The results for the random structure in Fig. 3 were simulated using an ensemble of supercells containing 512 C_{60} molecules. The HOMO, T_{1u} and T_{1g} densities of states have been broadened by 0.05, 0.15, and 0.15 eV half-widths respectively to mimic reported experimental resolution. Orientation randomness removes the sharp structures in the HOMO complex which exist in the two ordered crystal structures. However, the orientational disorder does not significantly change the widths of the DOS from those of the

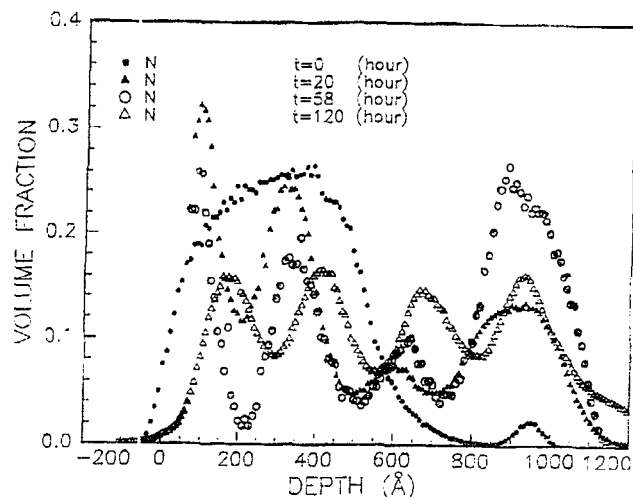


Figure 4: Density of states for solid C_{60} for a crystal with random molecular orientations, as given by LDA calculations, quasiparticle calculations, and as inferred from direct and inverse photoemission spectroscopy (PES and IPES). Experimental data are from Ref. 13.

$Fm\bar{3}$ structure. In fact, the DOS for the T_{1u} and the T_{1g} complexes are sharpened for the $Pa\bar{3}$ structure and the random structure. These trends are qualitative similar to those from a previous study [26].

The quasiparticle and LDA density of states are presented in Fig. 4 along with typical photoemission (PES) and inverse photoemission (IPES) data [13]. We note the remarkable improvement in agreement with PES/IPES results for the quasiparticle results as compared to LDA for both the minimum band gap and the $H_u - T_{1u}$ peak-to-peak distance. The present theory correctly calculates the excitation energies as the energies needed to add a quasiparticle or quasihole to the interacting many-electron system. Table I summarizes our results and data from various experiments. The calculated quasiparticle minimum gap is slightly small compared to values from PES/IPES [11-14], but too large compared to the result from microwave conductivity measurements [10]. The microwave conductivity results would in fact suggest a smaller $H_u - T_{1u}$ peak-to-peak distance leading to a better agreement between theory and experiment. There are also issues of the surface sensitivity of PES/IPES, sample characterization, or difficulty in aligning the electron chemical potentials in the separate PES and IPES experiments due to charging effects or sample damage in the latter case. Thus, the origin of the remaining discrepancy of 0.5 eV in the peak-to-peak distance remains uncertain.

We now examine the angle-resolved photoemission data and the issue of the band widths in solid C_{60} . Angle-resolved photoemission spectra were simulated, using the k -dependent DOS method described in Sec. II, for an ensemble of ten, randomly oriented 12×12 surface primitive cells which were 6 layer thick, oriented in the (111) direction. Such spectra could be compared to recently published ARPES results by Themlin *et al.* [17] which were obtained on epitaxially grown C_{60} films on a GeS(100) substrate. The simulated spectra in the $\bar{\Gamma} - \bar{K} - \bar{M}$ direction of the fcc (111) surface Brillouin zone are presented in Fig. 5a. We note that, even though there are 3 dispersing bands in the T_{1u} and the T_{1g} complexes, the calculated spectral peaks show negligible k_{\parallel} dependence. In Fig. 5b, we trace the dispersion of the theoretical peaks as compared with that reported by Themlin *et al.* Since the experimental energies are referenced to the Fermi level which was not known with respect to the valence band maximum, we have aligned in Fig. 5b the theoretical and experimental peak positions of the T_{1u} complex at $\bar{\Gamma}$.

The absence of strong, visible dispersion effects is seen in both theory and experiment, while the small visible dispersion is qualitatively similar in both sets. As finite energy or angular resolution in experiment or theory (due to the finite size of the supercell used), details of lifetime broadening, and small changes in our Slater-Koster fit would affect the results somewhat, more detailed comparison is difficult at present. Our quasiparticle results however clearly establish that the dispersive T_{1u} and T_{1g} states can lead to apparently non-dispersive ARPES spectra. We find that the absence of dispersion in the spectra is caused by several factors: orientational disorder, the required Brillouin-zone integration normal to the surface, finite-resolution effects, and the multi-band nature of the complexes studied. Thus, it would be incorrect to deduce that this is an extremely narrow-band system based solely on non-dispersive ARPES data. This subtlety has been discussed by others [16].

In addition to shedding light on the issue of dispersion, the quasiparticle results are in excellent agreement with experiment both in the peak widths and the peak-to-peak distance between the T_{1u} and T_{1g} complexes. This level of agreement is achieved only when the energy-dependent self-energy corrections are

Table I. Tabulated are the bandgap (E_g) and the $H_u - T_{1u}$ peak-to-peak interval, as given by direct and/or inverse photoemission (PES/IPES), microwave conductivity, LDA, and our quasiparticle (GW) calculation. All energies are in eV.

	PES/IPES	Microwave conductivity	LDA	Quasiparticle (GW)
E_g	2.3 ^a , 2.5 ^b , 2.6 ^c	1.85 ^d	1.04	2.15
$H_u - T_{1u}$ peak-to-peak	3.5 ^{a,b} , 3.7 ^c		1.6	3.0

a Ref. 13, b Ref. 12, c Ref. 14, d Ref. 10

included in the quasiparticle energies. As mentioned above, the corrections lead to an approximately 30% increase in the band widths and in the separation between the T_{1u} and T_{1g} complexes.

The effects of molecular orientational randomness [26] on the k-dependent density of states are illustrated in Fig. 6 for the T_{1u} states. We see that the delta-function spectrum at a given k-point for a perfect crystal is now significantly broadened. The large widths of the spectral peaks of the individual electronic states indicate a short mean-free-path of the electrons arising from scattering due to the molecular orientational disorders. It is the combined effects of this type of broadening with the multi-band nature of the complexes and k_{\perp} integration which give rise to the non-dispersive ARPES peaks.

Our calculations also show that, for the HOMO complex, the band nature of the electronic states may be seen in high-resolution angle-resolved photoemission experiments. Figure 7 depicts the calculated quasiparticle ARPES along $\bar{\Gamma}$ to \bar{M} in the fcc (111) surface Brillouin zone simulated using an ensemble of supercells containing 1536 molecules. The spectra were convoluted with a halfwidth of 0.05 eV to mimic typical experimental resolution. The width of the overall spectral distribution is in good agreement with experimental PES data. More importantly, the curves clearly demonstrate that there is a dispersion of a few tenths of an eV as one goes from $\bar{\Gamma}$ to \bar{M} . It should be noted that the theoretical results have neglected matrix elements and final state effects. These effects would alter the exact shapes of the observed spectra from those given by the simulation here. Recent high resolution

ARPES experiments by Gensterblum *et al* [27] have indeed observed dispersive features similar to those given in Fig. 8.

IV. Summary and Conclusions

We have carried out a study of the electron excitation energies in undoped, solid C_{60} within the theoretical framework of quasiparticles. For the Fm3 structure, an *ab initio* quasiparticle calculation was done using the method of Hybertsen and Louie within the GW approximation. A quantitative, tight-binding parameterization of our results has facilitated comparison of computed densities of states for crystals with a variety of orientational order or disorder, as well as comparison with angle-integrated and angle-resolved PES and IPES data. Using a quasiparticle picture in place of a LDA eigenvalue picture, we obtained substantial improvement in the agreement between theory and experiment for the band gap and the interval between the PES and IPES peaks closest to the gap. There is also a 30% increase in bandwidths compared to LDA results due to self-energy corrections. The theoretical results provide an explanation for the apparent lack of dispersion in the spectra peak positions observed in recent ARPES experimental on the unoccupied states. Moreover we show that the band nature of the HOMO complex should be observable in high-resolution ARPES. The present theory thus provides a quantitative description of many of the salient features in the experimental excitation spectra of solid C_{60} . Our results suggest that, although many-body corrections to the band gap and dispersion are sizable, the general electronic structure of this system is well described in a quasiparticle

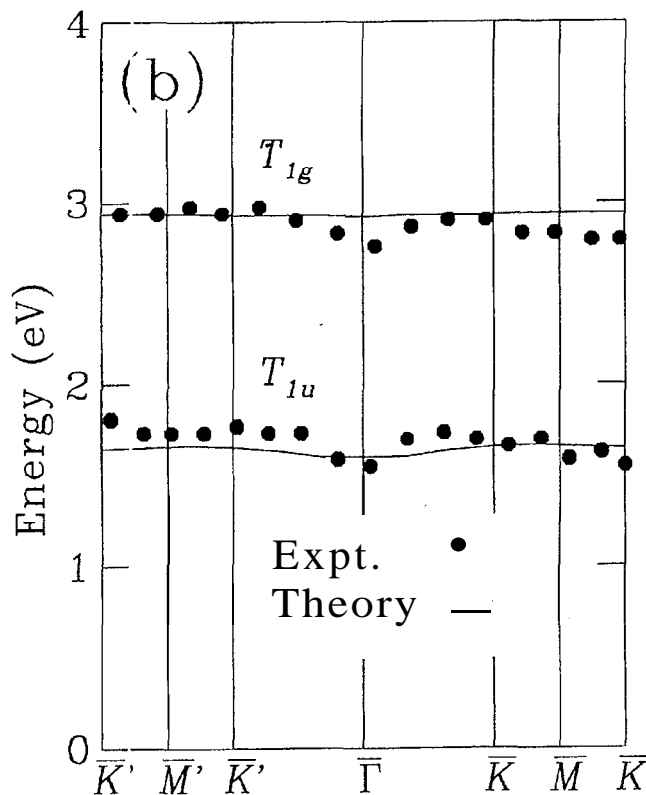
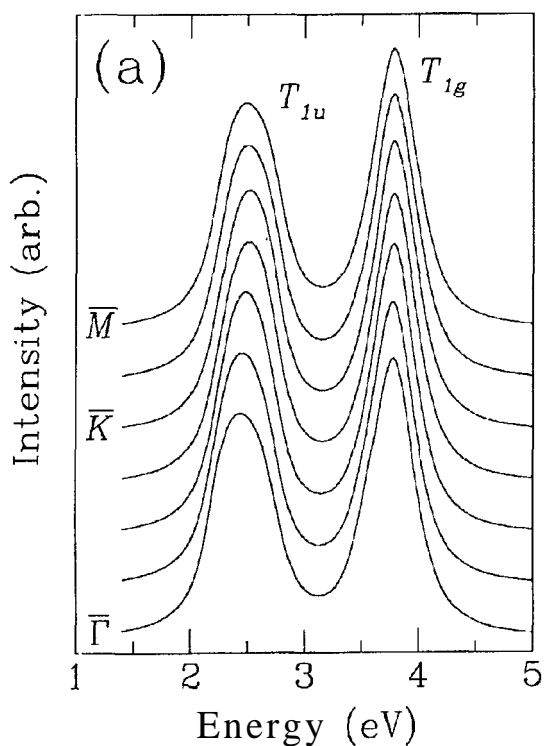


Figure 5: (a) Simulated ARPES spectra for solid C_{60} with random molecular orientations for the T_{1u} and T_{1g} complexes for various wavevectors k_{\parallel} in the (111) surface Brillouin zone; (b) dependence of spectral peak position on k_{\parallel} as given by our results (theory) and the experimental results of Ref. 17. The origin of the experimental energy scale is arbitrary, but this does not affect the $T_{1u} - T_{1g}$ splitting.

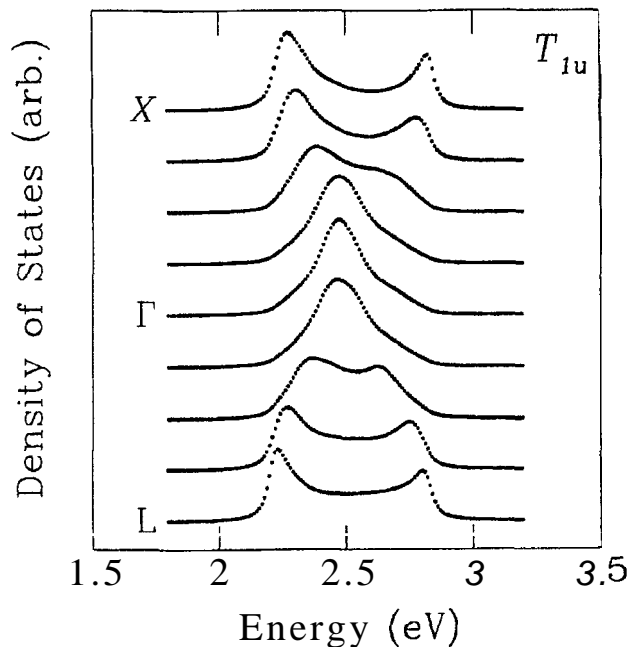


Figure 6: Calculated k-resolved density of states with meridional orientational randomness for the T_{1u} complex for various k-vectors along the $L - \Gamma - X$ direction in the bulk fcc Brillouin zone.

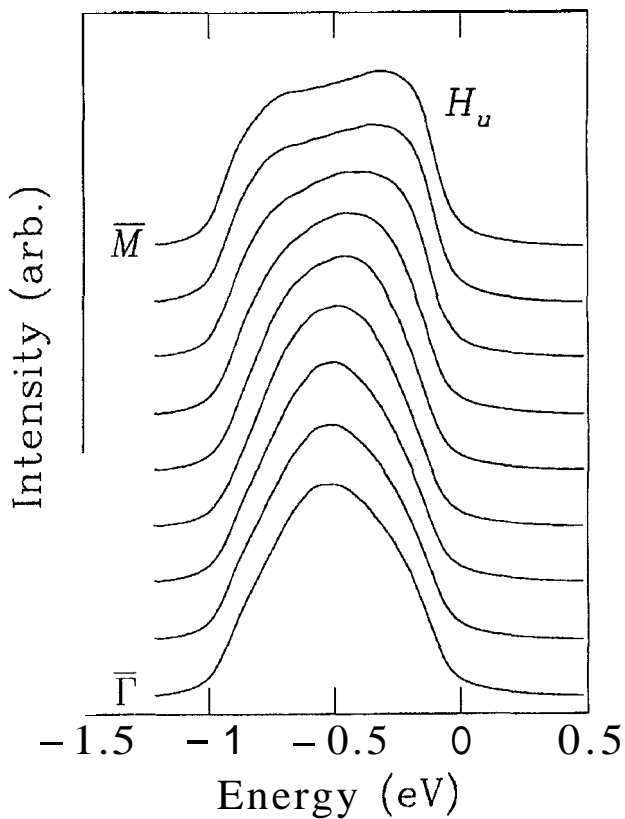


Figure 7: Simulated ARPES spectra for solid C_{60} with random molecular orientations for the HOMO complex along the $\bar{\Gamma} - \bar{M}$ direction in the (111) surface Brillouin zone.

band picture with molecular orientational disorder

Acknowledgments

This work was supported by National Science Foundation Grant No. DMR91-20269 and by the Director, Office of Energy Research, Office of Basic Energy Sciences, Materials Sciences Division of the U.S. Department of Energy under Contract No. DE-AC03-76SF00098. Supercomputer time was provided by the San Diego Supercomputer Center and by the National Energy Research Supercomputer Center. One of us (E.L.S.) acknowledges support by a fellowship of the Miller Institute for Basic Research in Science.

References

1. H. W. Kroto, J. R. Heath, S. C. O'Brien, R. F. Curl, and R. E. Smalley, *Nature* **318**, 162 (1985).
2. W. Kratschmer, K. Fostiropoulos, and D. R. Huffman, *Chem. Phys. Lett.* **170**, 167 (1990).
3. S. Iijima, *Nature* **354**, 56 (1991).
4. D. Ugarte, *Nature* **359**, 707 (1992).
5. A. F. Hebard *et al.*, *Nature* **350**, 600 (1991).
6. M. S. Hybertsen and S. G. Louie, *Phys. Rev. Lett.* **55**, 1418 (1985); M. S. Hybertsen and S. G. Louie, *Phys. Rev. B* **34**, 5390 (1986).
7. L. Hedin and S. Lundqvist, *Solid State Physics* **23**, *1*, edited by H. Ehrenreich, F. Seitz, and D. Turnbull (Academic, New York, 1969).
8. P. A. Heiney, J. E. Fischer, A. R. McGhie, W. J. Romanow, A. M. Denenstien, J. P. McCauley, A. H. Smith and D. E. Cox, *Phys. Rev. Lett.*, **66**, 2911 (1991); W. I. F. David, R. M. Ibberson, J. C. Matthewman, K. Prassides, T. J. S. Dennis, J. P. Hare, H. W. Kroto, R. Taylor, and D. R. M. Walton, *Nature* **353**, 147 (1991).
9. P. C. Hohenberg and W. Kohn, *Pliys. Rev.* **136**, B864 (1964); W. Kohn and L. J. Sham, *Pliys. Rev.* **140**, A1133 (1963).
10. T. Rabenau, A. Simon, R. K. Kremer, and E. Sohinen, *Z. Phys.* **B90**, 69 (1993).
11. P. J. Benning, J. L. Martins, J. H. Weaver, L. P. F. Chibante, and R. E. Smalley, *Science* **252**, 1417 (1991).
12. T. Takahashi, S. Suzuki, T. Morikawa, H. Katayama-Yoshida, S. Hasegawa, H. Inokuchi, H. Seki, K. Kikuchi, S. Suzuki, K. Ikemoto, and Y. Achiba, *Phys. Rev. Lett.* **68**, 1232 (1992).
13. R. W. Lof, M. A. van Veenendaal, B. Koopmans, H. T. Jonkman, and G. A. Sawatzky, *Phys. Rev. Lett.* **68**, 3924 (1992).
14. J. H. Weaver, *J. Pliys. Chem. Solids*, **53**, 1433 (1992).
15. J. C. Slater and G. F. Koster, *Phys. Rev.* **94**, 1498 (1954).
16. J. Wu, Z.-X. Shen, D. S. Dessau, R. Cao, D. S. Marshall, P. Pianetta, I. Landau, X. Yang, J. Terry, D. M. King, B. O. Wells, D. Elloway, H. R. Wendt, C. A. Brown, H. Hunziker, and M. S. de Vries, *Physica C*, **197**, 251 (1992).
17. J.-M. Themlin, S. Bouzidi, F. Coletti, J.-M. Debeyer, G. Gensterblum, Li-Ming Yu, J.-J. Pireaux, and P. A. Thiry, *Phys. Rev. B* **46**, 15602 (1992).
18. S. G. Louie in: *Electronic Structure, Dynamics and Quantum Structural Properties of Condensed Matter*, edited by J. Devreese and P. van Camp (Plenum, NY, 1985) p. 335.
19. D. M. Ceperley and B. J. Alder, *Phys. Rev. Lett.* **45**, 566 (1980); we use the parametrization given in J. P. Perdew and A. Zunger, *Phys. Rev. B* **23**, 5048 (1981).
20. D. R. Hamann, M. Schluter, and C. Chiang, *Phys. Rev. Lett.* **43**, 1494 (1979);
21. N. Troullier and J. L. Martins, *Phys. Rev. B* **46**, 1754 (1992).
22. Z. H. Levine and S. G. Louie, *Phys. Rev. B* **35**, 6310 (1982); M. S. Hybertsen and S. G. Louie, *Phys. Rev. B* **37**, 2733 (1988); X. Zhu and S. G. Louie, *Pliys. Rev. B* **43**, 14142 (1991).
23. X. Zhu and S. G. Louie, unpublished.
24. S. Satpathy, V. P. Antropov, O. K. Andersen, O. Jepsen, O. Gunnarsson, and A. I. Liechtenstein, *Phys. Rev. R* **46**, 1773 (1992).
25. R. Haydock, *Solid State Physics* **35**, 215, edited by H. Ehrenreich, F. Seitz, and D. Turnbull (Academic, New York, 1980).
26. M. P. Gelfand and J. P. Lu, *Phys. Rev. Lett.* **68**, 1050 (1992).
27. G. Gensterblum, J. J. Pireaux, P. A. Thiry, R. Caudano, T. Buslaps, R. L. Johnson, G. Lelay, V. Aristov, R. Gunter, A. Taleb, G. Indlekofer, and Y. Pctroff, preprint, 1993.